Vibrometer based on a self-mixing effect interferometer

L. Martí-López[a], R. González-Peña[b], R.A. Martínez-Celorio[c], and E.E. Ramírez-Miquet[a]
[a] *Centro de Aplicaciones Tecnológicas y Desarrollo Nuclear, Calle 30, no. 502 esq. 5ta. Miramar, La Habana. Cuba.*
[b] *Unidad Biofísica y Física Médica, Departamento de Fisiología, Facultad de Medicina, Universidad de Valencia, España.*
[c] *Grupo de Bioingeniería, DICIS, Universidad de Guanajuato, Salamanca, Guanajuato, México,*
e-mail: rcelorio@ugto.mx

Recibido el 30 de mayo de 2012; aceptado el 8 de agosto de 2012

We outline the basic principles of the self-mixing effect and present the design and construction of an interferometer based on this phenomenon. It differs from the previously reported in the literature by the use of two photodetectors, located at different arms of the interferometer. This feature allows widening the arsenal of strategies for the digital processing of the signal. The interferometer is used as vibrometer for the characterization of professional loudspeakers. Experimental results are presented as an illustration.

Keywords: Metrological applications; interferometers; techniques for non-destructive testing.

Se describen los principios básicos del efecto de automezclado y se presenta el diseño y la construcción de un interferómetro basado en este fenómeno que difiere de los reportes previos en la literatura por emplear dos fotodetectores, ubicados en los brazos diferentes del interferómetro. Esta propiedad permite ampliar el arsenal de estrategias para el procesamiento digital de la señal. El interferómetro es empleado para la caracterización de una bocina profesional. Los resultados experimentales se presentan a modo de ilustración.

Descriptores: Aplicaciones de metrología; interferómetros; técnicas de ensayos no destructivo.

PACS: 42.62.Eh; 07.60Ly; 43.40.Le

1. Introduction

Soon after the design and construction of the first laser by Maiman, back-reflection of laser light into the laser active medium was recognized as a serious perturbation source, affecting both amplitude and frequency of the emitted beam [1,2]. The amplitude and frequency fluctuations are due to a "parasite" feedback, other than the feedback by the mirrors of the laser resonator, caused by reflection (diffuse or not) on external surfaces. This phenomenon is called self-mixing effect. It is stronger in lasers with high-gain active media, as laser diodes. In most applications self-mixing effect is an undesirable effect that should be avoided by a careful optical design that includes the use of optical isolators. Self-mixing effect is related to injection locking and synchronization effects. The application of feedback-induced phenomena for measuring optical path lengths was reported as early as in 1968 [3]. The first example of a fringe-counting device based on a feedback interferometer was reported in 1978 [4]. Displacement measurements with $\lambda/2$ (or better resolution) [5-7], absolute distance measurements [8-10], velocimetry [11,12] and vibration measurement [13] have being demonstrated. On the other hand, Donati S. [14] described the basics principles of the self-mixing interferometers (*SMI*) and recently, the same author, presented updates and applications on *SMI* technique [15], where incorporated a differential SMI in a thermomechanical test equipment to determinate the mechanical hysteresis cycle of the beads of a motor-engine brake. In this paper we outline the basic principles of the self-mixing effect and present the design and construction of an interferometer based on this phenomenon for professional loudspeaker.

2. General considerations

Nowadays, a self-mixing interferometer (a feedback interferometer or an injection interferometer, all these terms are synonymous) is defined as an optical system performing a special type of detection, the so-called injection detection [16]. Injection detection is a special type of coherent detection, it may be homodyne (the self-mixing scheme) or heterodyne (the synchronization scheme) [16,17]. In both cases, injection detection can be used for measuring the phase and/or the amplitude of the signal. Thus, we can use injection detection to make a feedback interferometer and its variants for measuring displacement, speed, vibrations, optical path and related magnitudes.

The simplified scheme of a self-mixing interferometer with a laser diode is shown in Fig. 1. The photodiode is encapsulated inside the laser diode module. It senses the output

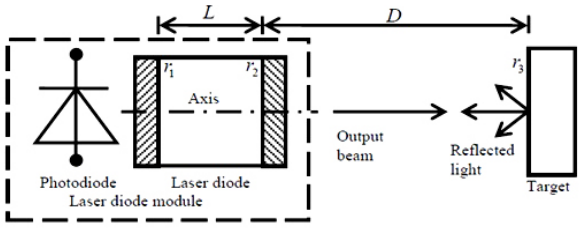

FIGURE 1. Simplified scheme of a self-mixing interferometer with a laser diode module with encapsulated photodiode. L is the length of the laser diode resonator, D - the distance from the front facet of laser diode to the target surface, and r_1, r_2 and r_3 - the coefficients of reflection of the rear facet, the front facet and the target, respectively.

power of the laser diode providing that way an electronic signal to the external circuitry. In most applications this signal is employed for output power stabilization by controlling the injection current via an electronic feedback.

The main features of a self-mixing interferometer with a laser diode, relevant to applications have been discussed elsewhere [17,18]. Here we present them with some comments based on our experience.

1. No external optical component to the source is needed. It results in a simple, reliable, compact and cheap setup. However, in some configurations, lenses and other optical components have to be added, for beam shaping or for increasing spatial resolution. These optical components may give some feedback perturbing that way the self-mixing detection.
2. No alignment is necessary, since the laser itself filters out spatially the spatial mode that interacts with the resonator mode. However, if the surface scatters light in a very narrow solid angle, alignment problems may arise because of the strong dependence of the feedback on the angle between the normal to the surface and the laser diode axis.
3. No external photodetector is needed, because the signal is provided by the monitor photodiode contained in the LD module. However, some of the technical characteristics of the encapsulated photodiode may be inadequate for a specific application. For example, its bandwidth may be not large enough to accommodate the Fourier spectrum of the signal. In such a case, an external photodetector and additional optical components must be added.
4. No stray-light filtering before the photodetector is needed. This is true when we use an encapsulated photodiode for light sensing.
5. The detector works always in the quantum regime, at the attainable SNR quantum-limit. It is true if we neglect the noise at the photodetector.
6. The beam can be sampled at different points, even at the same target.

3. Theory

In the three-mirror cavity model [17,18] the rear and the front facets of the laser diode (LD) and the target surface are considered as the mirrors of a laser resonator with reflection coefficients r_1, r_2, r_3, respectively. See Fig. 2. The optical beam is backscattered into the LD active resonator by the target, so that the laser operation is disturbed.

The optical power of the LD with external feedback P_c and the optical power without external feedback P_s are linked by the formula [17,18]:

$$P_c = P_s[1 + m' \cos(2\pi\nu_c\tau_{_D})] \tag{1}$$

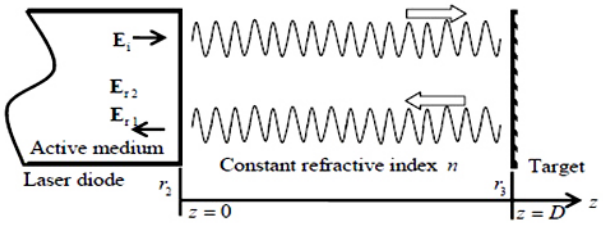

FIGURE 2. Scheme of the three mirror model of a self-mixing interferometer with a laser diode. E_i, E_{r1}, E_{r2} are the complex amplitudes of the incident and reflected electric waves at the interface front facet/air located at z = 0.

where: m', ν_c and $\tau_{_D}$ are the modulation parameter, the optical frequency of the emitted light with feedback and the round trip delay of photons, respectively. They are given by the expressions:

$$m' \approx \exp(-\pi\delta\nu_c\tau_{_D}), \tag{2}$$

$$\nu_c = \frac{\langle\omega_c\rangle}{2\pi} \tag{3}$$

$$\tau_{_D} = \frac{2nD}{c} \tag{4}$$

where, $\delta\nu_c$ is the bandwidth of the radiation with the external feedback, $\langle\omega_c\rangle$ - the mean angular frequency of the radiation with the external feedback, c - the speed of light in vacuum and n- the refractive index of the medium. Notice that the modulation parameter is not constant. It depends on the product $\delta\nu_c\ \tau_{_D}$. In turn, the bandwidth $\delta\nu_c$ depends also on τ_D through the expression [17]:

$$\delta\nu_c = \frac{\delta\nu_s}{[1 + c' \cos(2\pi\nu_c\tau_{_D} + \arctan\alpha)]^2} \tag{5}$$

where $\delta\nu_c$ is the bandwidth of the resonator without external feedback, c' is the modified feedback parameter, linked with the classical feedback parameter c by the expression:

$$c' = c\exp(-\pi\delta\nu_c\tau_{_D}) \tag{6}$$

and α is the bandwidth enhancement factor.

The classical feedback parameter is given by the expression:

$$c = \frac{\tau_{_D}}{\tau_{_L}}(1 - r_2^2)\frac{r_3}{r_2}(1 + \alpha^2)^{1/2} \tag{7}$$

where $\tau_{_L}$ is the round trip delay of photons inside the resonator.

For the case $c < 1$ (stable, single mode operation) the modulation parameter can be approximated as $m' \approx r_3$ [19]. Therefore the variations of the output power P_c are due to the changes of the optical path length *nD*.

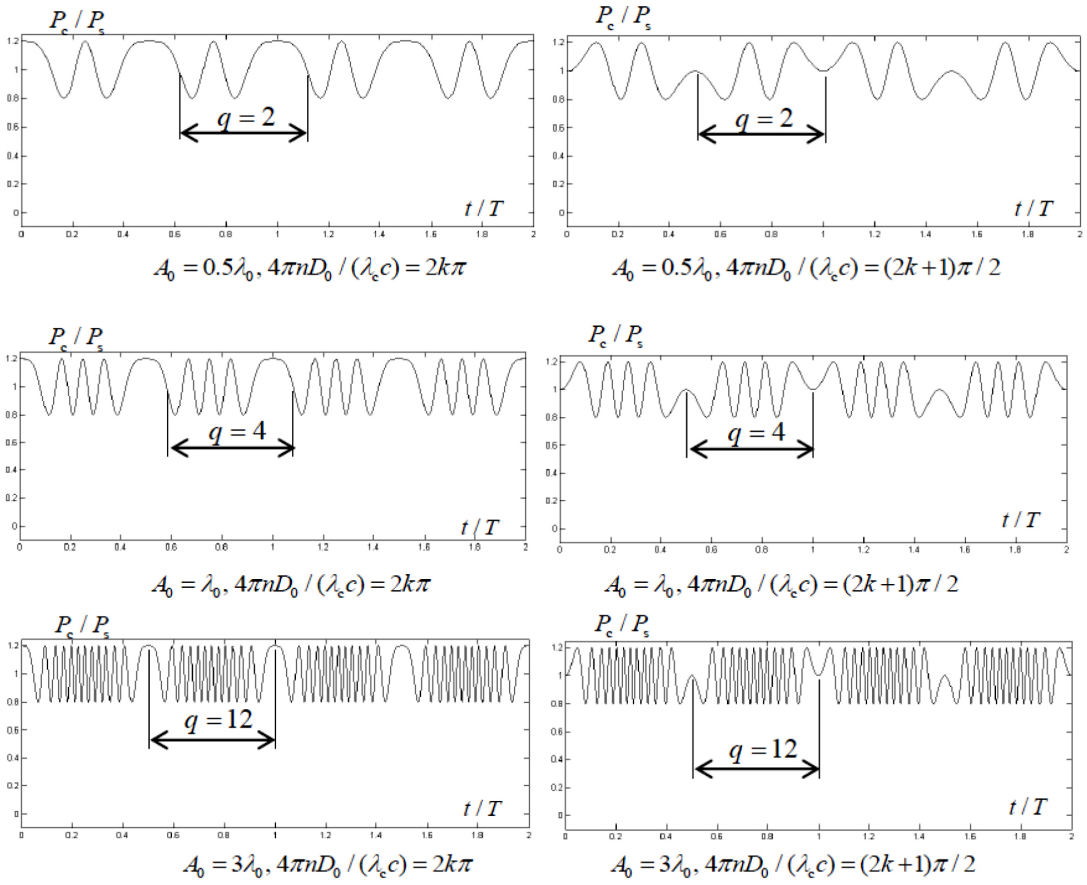

FIGURE 3. Plots of the normalized power from expression (9) versus normalized time. and k=0, ±1, ±2, ±3,...

4. Application to vibration measurement

Consider a sinusoidal vibration perpendicular to the target surface. Then the distance D can be written as:

$$D = D_0 + A_0 \cos\left(2\pi \frac{t}{T}\right) \tag{8}$$

where D is the mean position of the surface on the laser diode axis, A is the amplitude and T is the oscillation period.

Substituting the expression (8) into the expression (4) and the later into the expression (1) we obtain:

$$P_c = P_s \left\{ 1 + m' \times \cos\left[\frac{4\pi\nu_c n D_0}{c} + \frac{4\pi\nu_c n}{c} A_0 \cos\left(2\pi \frac{t}{T}\right)\right]\right\}$$

$$P_c = P_s \left\{ 1 + m' \times \cos\left[\frac{4\pi n D_0}{\lambda_c} + \frac{4\pi n}{\lambda_c} A_0 \cos\left(2\pi \frac{t}{T}\right)\right]\right\} \tag{9}$$

where $\lambda_c = c/\nu_c$ is the wavelength.

In the Fig. 3 function (3) is plotted for some values of its parameters.

To extract the amplitude from the expression (9) we can use different "tricks". The simpler one is to count the number of peaks q between two consecutive symmetrical points of the signal as shown in Fig. 3. From the expression (9) follows that the amplitude is

$$A_0 = \frac{q\lambda_c}{4} \tag{10}$$

with a relative uncertainty

$$\left|\frac{\Delta A_0}{A_0}\right| \leq \left|\frac{\Delta\lambda_c}{\lambda_c}\right| + \left|\frac{\varepsilon}{4q}\right| \tag{11}$$

where is the uncertainty of q, $0 < \varepsilon < 1$.

5. Vibrometer

In Fig. 4 a simplified scheme of the self-mixing interferometer is shown. Its component blocks are as follows.

1. Optical block. The laser diode module (1) HL6738MG (35 mW, 680 nm, single mode, from Hitachi) contains the photodiode (2) and the laser diode (3). Both devices are fed by a stabilized power supply (model

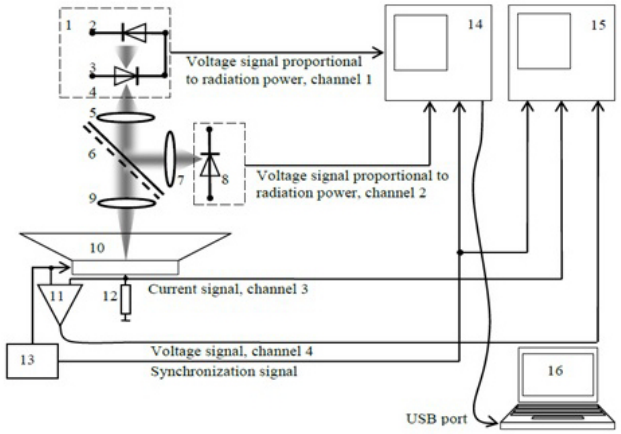

FIGURE 4. Simplified scheme of the interferometer.

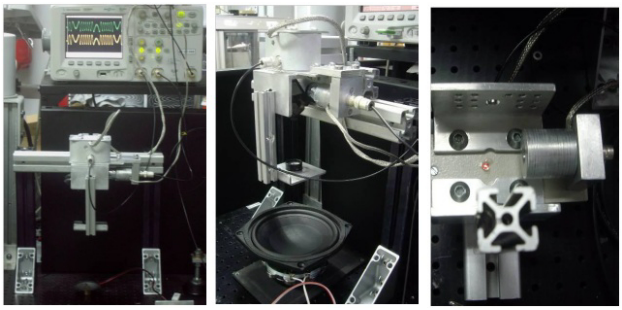

FIGURE 5. Laser vibrometer. Front view (left), Focusing lens and loudspeaker (medium) and Laser diode with beam shaping optics and photodiode in its housing (right).

IPS4303 from Isotech) and have an ad hoc circuitry, not shown in Fig. 4. The large divergence in the fast axis of the beam (4) is corrected by the beam shaping optics (5) to obtain a collimated beam. The 50% beam splitter (6) samples the beam, sending a fraction to the collecting lens (7), which in turn focuses it on the photodetector (8). The photodetector (8) is a commercially available photodiode with an ad hoc circuitry, not shown in Fig. 4. The lens (9) focuses the beam on the surface of a professional loudspeaker (10).

2. Electronic block. The voltage differential amplifier (11) senses the input voltage delivered by the function generator (13) (model GFG 8216A from Isotech) to the loudspeaker. The resistance (12) (R=1Ω±1%) samples the current flowing through the loudspeaker. The signals coming from the photodiode 1 (PHD 1, channel 1), the photo-diode 2 (PHD 2, channel 2), are introduced into the dual trace digital oscilloscope (14) (model DSO 6052A from Agilent), while the current signal (channel 3) and the voltage signal (channel 4) – to the dual trace oscilloscope (15) (model PM 3335 from Philips). If we want to record digitally the current and voltage signals, the channel 3 and 4 are connected to the oscilloscope (14) and the channels 1 and 2 to the oscilloscope (15). Other connection schemes are possible. A TTL synchronization signal from the function generator (13) is introduced into the oscilloscopes (14) and (15) for obvious purposes. The digital signals at the oscilloscope (14) can be saved as images, ASCII files or excel files in a personal computer (16) or in a flash memory via the USB port.

The interferometer is mounted on a homemade optical table isolated from external vibrations and sounds.

6. Signal processing

Assuming a linear response of the photodetector and a negligible signal distortion, the captured signal has the form:

$$V(t) = V_0 \cos[4\pi D_n + 4\pi A_n \cos(2\pi t_n + \varphi_0)] \qquad (12)$$

where: V_0 and φ_0 are the amplitude and the initial phase, respectively, $D_n = D_0/\lambda_c$, $A_n = A_0/\lambda_c$, $t_n = t/T$ – the normalized mean position of the surface, the normalized amplitude and the normalized time, respectively, and $n = 1$ was assumed. The DC term occurring in expression (9) was dropped because we keep the AC component only.

From the expression (12) follows that numerical techniques of phase unwrapping should be applied to extract the amplitude. Here we describe a simpler but not so precise technique to extract the amplitude. The main drawback of the counting method is that the relative uncertainty of $q, \varepsilon/q$ approaches to unity as the amplitude tends to zero. To palliate it let us consider the recurrence transformation:

$$f_{g+1} = 2(f_g^2 - 0.5) \qquad (13)$$

where $g = 1, 2, 3, \ldots$ and

$$f_1 = \cos[4\pi D_n + 4\pi A_n \cos(2\pi t_n + \varphi_0) \qquad (14)$$

Notice that the function f_1 is the normalized captured signal $V(t)$ (12). Figure 7 illustrates the effect of the recurrence transformation (13) on f_1.

It can be shown that the number of peaks Q_g of function f_g is $Q_g = 2^{g-1}q$ where q is the number of peaks of the function f_1. Consequently, the amplitude can be calculated as

$$A_0 = \frac{Q_g \lambda_c}{2^{g+1}} \qquad (15)$$

This procedure has two advantages. First, the peaks of the function f_g, $g > 1$, are narrower than the peaks of the function f_1; it reduces the uncertainty of the peak counting. Second, peak counting on the function f_g reduces uncertainty propagation to the amplitude. To show the latter we consider that for peak counting on function f_g, the relative uncertainty of the amplitude is:

$$\left|\frac{\Delta A_0}{A_0}\right| \leq \left|\frac{\Delta \lambda_c}{\lambda_c}\right| \leq \left|\frac{\varepsilon}{2^{g+1} Q_g}\right| \qquad (16)$$

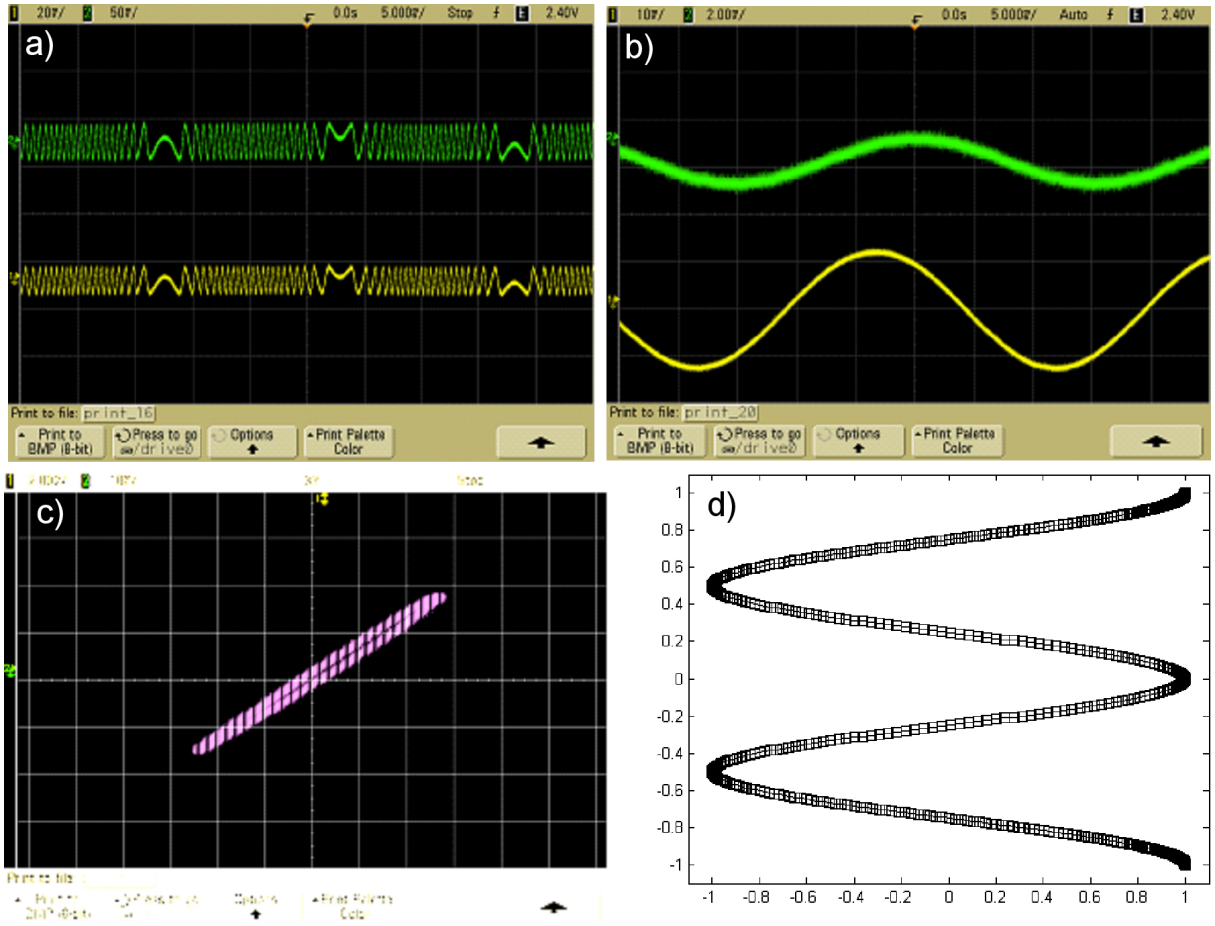

FIGURE 6. Signals from the Beyma loudspeaker shown in Fig. 5, excited at f=32.7 Hz. a) $A_0 = 6\lambda_c = 4.1$ μm. $\pm$ 5 % green trace – PHD 2, Yellow trace – PHD1. b)Signals from the loudspeaker. Green trace: current signal, yellow trace: voltage signal. c) Lissajous figure of the signals from the loud-speaker. X axis – voltage signal, Y axix – current signal. d) Lissajous figure of the signals from the loudspeaker. X axis – normalized current signal, Y axis normalized signal PHD1.

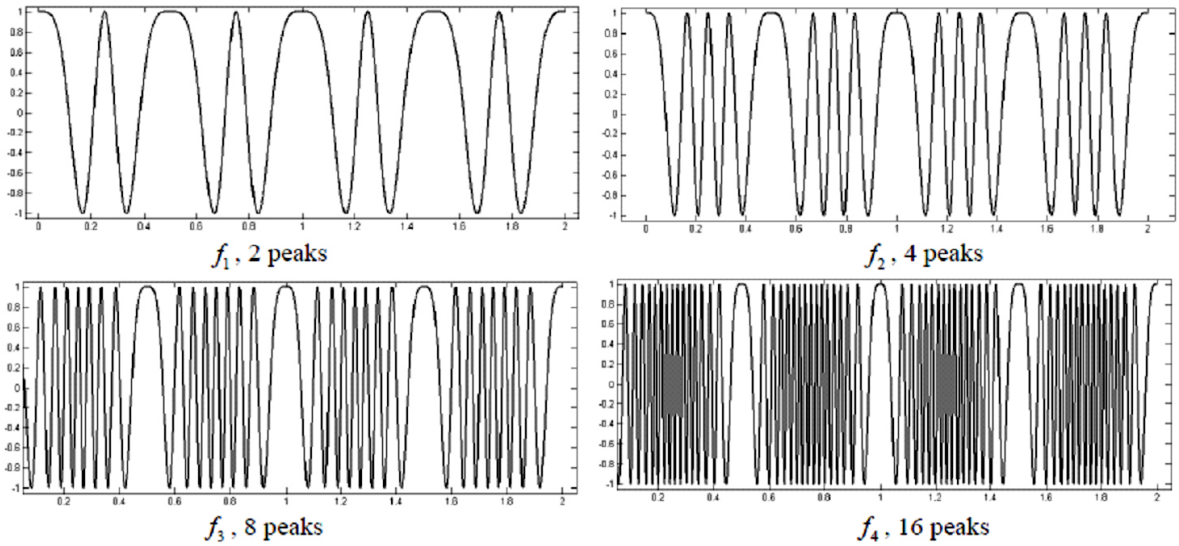

FIGURE 7. Recurrence transformations for $A_0 = 0.5\lambda_c$.

Assuming a similar uncertainty ε for Q_g we obtain a reduction of the contribution of the counting to the amplitude uncertainty of $2^{-g+1}q/Q_g$. For $g > 3$ the contribution of the relative uncertainty of peak counting to the relative uncertainty (16) is negligible. Since the typical relative wavelength uncertainty is $|\Delta\lambda_c|/\Delta\lambda_c \leq 0.01$ we may expect an amplitude uncertainty $|\Delta A_0|/A_0 \leq 0.01$. Peak counting works well for $A_n \geq 0.5$ with the described procedure. For smaller vibration amplitudes unwrapping techniques should be used.

7. Conclusions

A laser vibrometer based on the self-mixing effect in an LD has been demonstrated. A prototype instrument has been designed, built and tested in the vibration measurement of professional loudspeakers. In addition, a variant of the peak counting method for amplitude measurement have been described. The self-mixing laser vibrometer can find application cases where non-contact operation is required, for monitoring of soft or lightweight structures. Other applications involve vibration measurement of delicate biological objects such as the tympanic membrane. The proposed laser vibrometer is intrinsically low cost since it is made of simple, off-the-shelf optical components, and uses a straightforward signal processing, owing to the simplicity and effectiveness of the self-mixing interferometric scheme. In the near future we plan to improve the technical characteristics of the presented prototype to increase its sensibility and accuracy.

Acknowledgments

This work was carried out with support of the Asociación Industrial de Óptica, Color e Imagen (AIDO) and of the Centro de Tecnologías Aplicadas y Desarrollo Nuclear (CEADEN). *RAMC* would like to thank the *Universitat de València* for the support and access given to its facilities.

1. M.B. Spencer and W.E. Lamb, Jr., *Phys. Rev. A* **5** (1972) 884–897.
2. M.B. Spencer and W.E. Lamb, Jr., *Phys. Rev. A* **5** (1972) 898–912.
3. M.J. Rudd, *J. Sci. Instrum.* **1** (1968) 723– 726.
4. S. Donati, *J. Appl. Phys.* **49** (1978) 495–497.
5. S. Donati, L. Falzoni, and S. Merlo, *IEEE Trans. Instrum. Meas.* **45** (1996) 942–947.
6. P.A. Roos, M. Stephens, and C.E. Wieman, *Appl. Opt.* **35** (1996) 6754–6761.
7. S. Merlo and S. Donati, *IEEE J. Quantum Electron.* **33** (1997) 527–531.
8. G. Beheim and K. Fritsch, *Appl. Opt.* **25** (1986) 1439–1442.
9. S. Shinohara, H. Yoshida, H. Ikeda, K. Nishide, and M. Sumi, *IEEE Trans. Instrum. Meas.* **41** (1992) 40–44.
10. P.J. de Groot, G. M. Gallatin, and S. H. Macomber, *Appl. Opt.* **27** (1988) 4475–4480.
11. T. Shibata, S. Shinohara, H. Ikeda, H. Yoshida, T. Sawaki, and M. Sumi, *IEEE Trans. Instrum. Meas.* **45** (1996) 499–503.
12. W.M. Wang, K. T. V. Grattan, A. W. Palmer, and W. J. O. Boyle, *J. Lightwave Technol.* **12** (1994) 1577–1587.
13. G. Giuliani, S. Bozzi-Pietra and S. Donati, *Meas. Sci. Technol.* **14** (2003) 24–32.
14. S. Donati, *Electro-Optical Instrumentation - Sensing and Measuring with Lasers*, (Ed. Prentice Hall, USA, ISBN) **013** (2004) 0161610-9.
15. S. Donati, *Laser Photonics Rev.* 1–25 (2011). **DOI**10.1002/lpor.201100002.
16. S. Donati, *Photodetectors, Devices, Circuits and Applications* Chapter 8, (Prentice Hall, Upper Saddle River, NJ 2000).
17. T. Bosch, N. Servagent and S. Donati, *Opt. Eng.* **40** (2001) 20–27.
18. G. Giuliani, M. Norgia, S. Donati and T. Bosch, *J. Opt. A: Pure Appl. Opt.* **4** (2002) S283–S294.
19. G. Mourat, N. Servagent, and T. Bosch, *Opt. Eng.* **39** (2000) 738–743.